DALTON
FULL PAPER

Thermo-Raman investigations on thermal decomposition of $(NH_4)_6Mo_7O_{24}\cdot 4H_2O$

Ramaswamy Murugan † and Hua Chang *

Department of Chemistry, National Tsing Hua University, Hsinchu, Taiwan 30034, Republic of China

Received 2nd April 2001, Accepted 10th August 2001
First published as an Advance Article on the web 27th September 2001

An extensive study by thermo-Raman spectroscopy was carried out to understand the structural changes occurring during the thermal decomposition of $(NH_4)_6Mo_7O_{24}\cdot 4H_2O$ in open air and under O_2 and N_2 flow. In addition, themogravimetry, differential thermal analysis and thermogravimetry coupled with mass spectrometry analysis were also carried out and a satisfactory decomposition mechanism has been proposed on a molecular level. The thermo-Raman investigations on the decomposition of $(NH_4)_6Mo_7O_{24}\cdot 4H_2O$ or $12(NH_4)_2O\cdot 4(MoO_3)_7\cdot 16H_2O$, since there are four formulae in a unit cell, in open air indicated the formation of a first intermediate $11(NH_4)_2O\cdot 4(MoO_3)_7$ in the temperature interval from 124 to 131 °C and a second intermediate $7(NH_4)_2O\cdot 4(MoO_3)_7$ from 174 to 239 °C, the coexistence of a third intermediate (mixed molybdena with residual volatile components) with MoO_3 from 255 to 346 °C and the formation of MoO_3 from 347 °C onwards. The present investigations indicated that during the thermal decomposition process from 25 to 250 °C, the $(MoO_3)_7$ unit in $(NH_4)_6Mo_7O_{24}\cdot 4H_2O$ remained intact and the collapse of $(MoO_3)_7$ occurred to form MoO_3 immediately subsequent to the loss of the remaining volatile compounds at 255 °C. The thermal decomposition of $(NH_4)_6Mo_7O_{24}\cdot 4H_2O$ under O_2 and N_2 flow was also investigated in detail.

Introduction

Hexaammonium heptamolybdate tetrahydrate $(NH_4)_6Mo_7O_{24}\cdot 4H_2O$ is usually used as the basic source for the preparation of molybdenum containing catalysts.[1] The industrial importance of molybdena as a catalyst has promoted a large number of characterization studies on the active phase of this catalyst since the catalytic performance depends heavily on the structure of the active phase, which is directly influenced by preparation processes such as drying, thermal decomposition and calcination. Several spectroscopic techniques[2–8] including Raman spectroscopy[9–12] and thermal analysis like thermogravimetry (TG)[13] and differential thermal analysis (DTA)[14] were used to derive structural information during catalyst preparation. Raman spectroscopy has contributed a lot to the progress in this area of catalysis because of its *in situ* capabilities and its ability to identify different metal oxide structures.[9–12] Although several techniques are available there is still a lack of reliable practical techniques to follow the catalyst preparation process dynamically.

As a key catalyst material $(NH_4)_6Mo_7O_{24}\cdot 4H_2O$ continues to inspire new research efforts to better understand its thermal decomposition. Extensive studies on the thermal decomposition of $(NH_4)_6Mo_7O_{24}\cdot 4H_2O$ by TG, DTA, XRPD, ammonia determination and omegatron mass-spectrometry were carried out earlier by Ma.[13,14] Based on the experimental results, Ma proposed that it decomposed into $2(NH_4)_2O\cdot 5MoO_3$ at around 115 to 130 °C then to $2(NH_4)_2O\cdot 8MoO_3$ at around 225 to 245 °C and finally to MoO_3 at around 320 to 355 °C.[13,14] On the basis of TG and DTA data, Erdey *et al.* proposed that $(NH_4)_6Mo_7O_{24}\cdot 4H_2O$ dehydrated into $(NH_4)_6Mo_7O_{24}$ at around 40 to 170 °C then decomposed to $6NH_3\cdot 7MoO_3$ at around 170 to 260 °C and finally to MoO_3 at around 400 °C.[15] Based on high temperature XRD and TGA/DTA data, Zhoulan *et al.* proposed that $(NH_4)_6Mo_7O_{24}\cdot 4H_2O$ decomposed and gave off NH_3 to form a series of ammonium molybdates such as $(NH_4)_4Mo_5O_{17}$, $(NH_4)_2Mo_4O_{13}$ and finally MoO_3 in sequence.[16,17] The thermal decomposition of $(NH_4)_6Mo_7O_{24}\cdot 4H_2O$ was also studied by Kiss and Gado and they proposed formation of intermediates $(NH_4)_2Mo_{14}O_{43}$ and $(NH_4)_2Mo_{22}O_{67}$.[18] Li *et al.* studied the thermal decomposition of $(NH_4)_6Mo_7O_{24}\cdot 4H_2O$ using FT-IR emission spectroscopic techniques and could identify only dehydration and deammoniation processes.[3] Although studies on the thermal decomposition of $(NH_4)_6Mo_7O_{24}\cdot 4H_2O$ were extensive, a satisfactory and detailed decomposition mechanism especially at molecular level is still lacking.

Thermo-Raman spectroscopy (TRS) in which Raman spectra are measured dynamically as a function of temperature has been applied successfully in the *in situ* investigation of solid state phase transformations and composition changes.[19–25] It can monitor dynamically the thermal decomposition of $(NH_4)_6Mo_7O_{24}\cdot 4H_2O$ *in situ* in 1 °C resolution. Hence, in this work TRS studies were carried out to understand the thermal decomposition mechanism of $(NH_4)_6Mo_7O_{24}\cdot 4H_2O$ in open air and under O_2 and N_2 flow. In addition, TG, DTA and TG-MS (thermogravimetry coupled with mass spectrometry) analyses were also carried out to support the thermal decomposition mechanism revealed by TRS.

Experimental

Hexaammonium heptamolybdate tetrahydrate $(NH_4)_6Mo_7O_{24}\cdot 4H_2O$ (Riedel-deHaen) was used without further purification. Raman scattering was excited with an argon ion laser (Coherent, Innova 100–15) operating at a wavelength of 514.5 nm. The scattered radiation was collected, analyzed by a 0.5 m spectrophotometer (Spex) and detected by a CCD camera (Princeton Instruments, 1024 × 1024 pixels). Spectra were taken continuously with 12 seconds exposure time such that each spectrum covered 1 °C in a dynamic thermal process heating from 25 to 500 °C with a 5 °C min^{-1} heating rate in open air and under O_2 and N_2 flow (in a home-made sample cell) under

† On leave from Department of Physics, Pondicherry Engineering College, Pondicherry, 605 014, India.

DOI: 10.1039/b102959m

irradiation of low laser power of 20 mW for thermo-Raman studies. The spectra were calibrated using an argon lamp and the resolution was about 2 cm^{-1}.

TG and DTA (Seiko I SSC 5000 TGA/DTA) thermograms were recorded under air and N_2 flow with a flow rate of 100 mL min^{-1}. Combined TG, DTA (Seiko I SSC 5000 TGA/DTA) thermograms of $(NH_4)_6Mo_7O_{24}\cdot 4H_2O$ and traces of evolved gases sampled by a mass spectrometer (VG quadrupoles micromass spectrometer) were also recorded simultaneously under He flow with a flow rate of 100 mL min^{-1}. A TG (Perkin Elmer TGA6) thermogram was also recorded in O_2 flow with a flow rate of 100 mL min^{-1}. All the thermograms were taken under the same thermal process from 25 to 500 °C with a 5 °C min^{-1} heating rate.

Results

Thermo-Raman spectroscopy (TRS)

Although there have been a number of studies on the assignment of Raman bands of $(NH_4)_6Mo_7O_{24}\cdot 4H_2O$ supported on metal oxides,[9,11,12] there were disagreements on the interpretation of the Raman bands. However, Raman studies on the thermal decomposition of unsupported $(NH_4)_6Mo_7O_{24}\cdot 4H_2O$ were scarce. The changes in the spectral profile observed by TRS in 1 °C intervals in this work would indicate in detail the variation in composition during the thermal decomposition of $(NH_4)_6Mo_7O_{24}\cdot 4H_2O$.

In open air

MoO_6 vibrations. For MoO_6 having O_h symmetry, six fundamental vibrations, symmetric stretching $\nu_1(A_{1g})$, asymmetric stretching $\nu_2(E_g)$ and $\nu_3(F_{1u})$, asymmetric bending $\nu_4(F_{1u})$, symmetric bending $\nu_5(F_{2g})$ and inactive $\nu_6(F_{2u})$ modes, were interpreted.[26] In a crystalline environment, the octahedral symmetry of MoO_6 is lowered by the sharing of oxygen atoms with other groups. Since there were different Mo–O distances and different Mo–O–Mo angles in the $(NH_4)_6Mo_7O_{24}\cdot 4H_2O$ crystalline environment, the Raman spectra in the terminal Mo–O and bridging Mo–O–Mo vibration regions became complicated with different frequencies for different Mo–O distances and Mo–O–Mo angles. Hardcastle criteria[27] and earlier investigations[9] on $(Mo_7O_{24})^{6-}$ indicated that stretching vibrations of terminal Mo–O bonds were at higher frequencies in the range from 1000 to 890 cm^{-1}. The earlier analysis also indicated that stretching vibrations of Mo–O–Mo bridge bonds occurred from 850 to 500 cm^{-1}, frequencies lower than those of terminal bonds.[9] The deformation modes of terminal Mo–O and bridging Mo–O–Mo bonds usually appeared below 500 cm^{-1}, however it was rather difficult to analyze because these modes were observed together with the librational modes of NH_4^+ and H_2O.

In this work, 475 Raman spectra were taken, there were three major and three minor changes. Seven typical thermo-Raman spectra observed at 25, 115, 140, 200, 245, 275 and 385 °C during the thermal decomposition of $(NH_4)_6Mo_7O_{24}\cdot 4H_2O$ in open air in the terminal Mo–O and bridging Mo–O–Mo stretching region are illustrated in Fig. 1. The variation in thermo-Raman spectra during these changes is not shown. Band positions and their tentative vibrational assignments are presented in Table 1. As reported, a strong band at 934 cm^{-1} due to the symmetric stretching of the short Mo–O terminal bond along with medium bands at 890 and 881 cm^{-1} and weak bands at 905, 859 and 838 cm^{-1} was observed for the room temperature Raman spectrum as shown in Fig. 1(a). Thermo-Raman spectra measured in this range indicated no major change until 74 °C. However from 75 to 115 °C several minor changes in the weak bands were found but the strongest band at 934 cm^{-1} remained the same. A typical thermo-Raman spectrum measured at 115 °C is shown in Fig. 1(b). This is the first minor change in the Raman spectra.

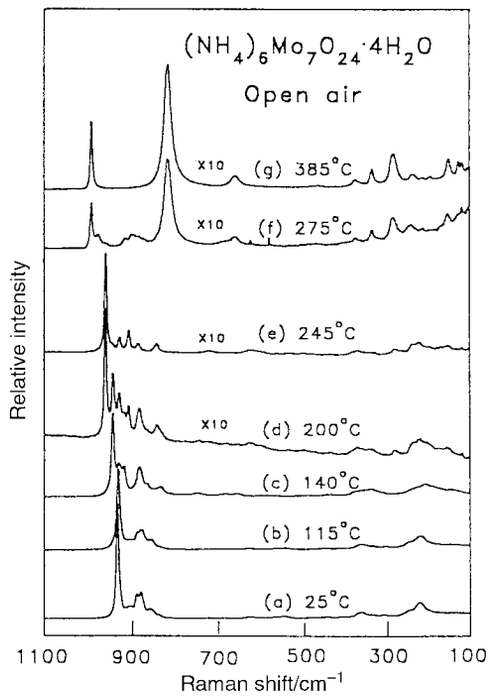

Fig. 1 Typical thermo-Raman spectra of $(NH_4)_6Mo_7O_{24}\cdot 4H_2O$ in open air in the 100 to 1100 cm^{-1} region in a dynamical thermal process. (a) $(NH_4)_6Mo_7O_{24}\cdot 4H_2O$, at room temperature, (b) $(NH_4)_6Mo_7O_{24}\cdot xH_2O$, after the onset of dehydration, (c) $11(NH_4)_2O\cdot 4(MoO_3)_7$, the first intermediate, (d) mixture of $11(NH_4)_2O\cdot 4(MoO_3)_7$, the first intermediate, and $7(NH_4)_2O\cdot 4(MoO_3)_7$, the second intermediate, (e) $7(NH_4)_2O\cdot 4(MoO_3)_7$, the second intermediate, (f) MoO_3 and the third intermediate and (g) MoO_3.

Besides some minor changes, the major spectral variation observed in the TRS indicated the appearance of a band at 945 cm^{-1} from 121 °C and also an increase in its intensity with temperature. Although the intensity of the strong band at 934 cm^{-1} decreased considerably during this temperature interval still it appeared as a weak band even at 133 °C but slightly shifted to 931 cm^{-1}. A typical thermo-Raman spectrum measured at 140 °C is shown in Fig. 1(c). This was the first major change observed in the Raman spectra from 121 to 133 °C.

The appearance of a band at 961 cm^{-1} from 176 °C and its increase in intensity with temperature were notable spectral variations observed in the next temperature range in the TRS for the second major change. The intensity of the strong band at 945 cm^{-1} decreased from 176 °C but it still appeared as a weak band even at 231 °C. The bands observed at 931 and 919 cm^{-1} at 140 °C were slightly shifted to 929 and 918 cm^{-1}, respectively, at 199 °C. Therefore, a second major change was the replacement of the band at 945 cm^{-1} by that at 961 cm^{-1} from 176 to 231 °C and the second minor change was the disappearance of the band at 945 cm^{-1} from 232 to 255 °C. Typical thermo-Raman spectra measured at 200 and 245 °C are shown in Figs. 1(d) and (e), respectively.

The interesting spectral variation observed in the next temperature interval was the appearance of the characteristic Raman bands of MoO_3 at 993, 819 and 664 cm^{-1} from 255 °C. In addition, a weak band at 977 cm^{-1} appeared from 255 °C and its intensity increased slightly with temperature up to 305 °C but then decreased. The intensity of the strong band at 961 cm^{-1} decreased from 250 °C and disappeared at around 275 °C. Several weak bands observed at around 245 °C were replaced by three broad weak bands centered at 917, 902 and 884 cm^{-1} at around 275 °C as shown in Fig. 1(f). This is the third major variation. An appreciable decrease in intensities of those weak

Table 1 Band positions (in cm^{-1}) and their tentative vibrational assignments of the Raman spectrum of $(NH_4)_6Mo_7O_{24}\cdot 4H_2O$ from 800 to 1000 cm^{-1} during dynamical thermal processes

25 °C[c]	115 °C[d]	140 °C[e]	200 °C[f]	245 °C[g]	275 °C[h]	385 °C[i]
					993(m)[a]	992(s)[a]
					977(w)[a]	
			961(s)[a]	961(s)[a]		
		945(s)[a]	945(m)[a]	945(vw)[a]		
934(vs)[a]	934(vs)[a]					
		931(w)[a]	929(w)[a]	929(w)[a]		
		919(w)[a]	918(vw)[a]		917(vw)[a]	
			910(vw)[a]	910(w)[a]		
905(vw)[a]					902(w)[a]	
890(m)[a]	890(w)[a]					
		884(m)[a]	884(m)[a]	884(m)[a]	884(vw)[b]	
881(m)[a]	881(w)[a]					
		866(vw)[b]	866(vw)[b]			
859(w)[b]	859(w)[b]					
		850(vw)[b]	850(vw)[b]	850(vw)[b]		
			844(w)[b]	844(w)[b]		
838(vw)[b]	838(vw)[b]	836(vw)[b]				
					819(s)[b]	819(vs)[b]

vs very strong, s strong, m medium, w weak and vw very weak. [a] ν(Mo–O). [b] ν(Mo–O–Mo). [c] $(NH_4)_6Mo_7O_{24}\cdot 4H_2O$ or $3(NH_4)_2O\cdot(MoO_3)_7\cdot 4H_2O$, original sample. [d] $(NH_4)_6Mo_7O_{24}\cdot xH_2O$ (after onset of dehydration). [e] $11(NH_4)_2O\cdot 4(MoO_3)_7$, the first intermediate. [f] Mixture of $11(NH_4)_2O\cdot 4(MoO_3)_7$, the first intermediate, and $7(NH_4)_2O\cdot 4(MoO_3)_7$, the second intermediate. [g] $7(NH_4)_2O\cdot 4(MoO_3)_7$, the second intermediate. [h] MoO_3 and the third intermediate (mixed molybdena with residual volatile compounds). [i] MoO_3.

bands from 310 °C and their complete disappearance at around 347 °C were also observed. The increase in intensities of characteristic Raman bands of crystalline MoO_3 above 350 °C was clear. A typical thermo-Raman spectrum measured at 385 °C corresponding to MoO_3 is shown in Fig. 1(g). This was the third minor change. The similarity of the spectra observed in the terminal Mo–O and bridging Mo–O–Mo stretching regions (Figs. 1(a)–(g)) indicated that no major change occurred in the skeleton structure of $(MoO_3)_7$ from 25 to 250 °C, however it dramatically changed at around 255 °C to form MoO_3. From the thermo-Raman spectra, there were three intermediates with the Raman spectra shown in Figs. 1(c), (e) and (f) corresponding to the three major variations in the spectra.

NH_4^+ and H_2O vibrations. The normal modes of free NH_4^+ under T_d symmetry have frequencies at 3033, 1689, 3134 and 1397 cm^{-1} for $\nu_1(A_1)$, $\nu_2(E)$, $\nu_3(F_2)$ and $\nu_4(F_2)$ modes, respectively.[26] All the modes are Raman active. Since NH_4^+ in $(NH_4)_6Mo_7O_{24}\cdot 4H_2O$ occupy sites of lower symmetry than those of the free ion, anisotropic crystal fields may remove the degeneracies of the normal modes. The normal modes of H_2O are at 3651 (ν_1), 1595 (ν_2) and 3755 (ν_3) cm^{-1}.[26] In the last two decades, there has been growing interest in understanding the nature and role of crystalline water in hydrated crystals. In this compound, NH_3 and H_2O are both involved in stabilizing the structure. In general, the anion–water interaction involving hydrogen bonding affords stability to the hydrated materials. The Raman spectra of water in hydrated crystals usually show extremely broad bands, making interpretation difficult.

A broad band at 3491 cm^{-1} and a weak shoulder at 3329 cm^{-1} due to the stretching modes of H_2O and a strong band at 3141 cm^{-1} due to the stretching modes of NH_4^+ and a weak band at 2795 cm^{-1} possibly due to the overtone of the ν_4 mode of NH_4^+ were observed in the room temperature spectrum of $(NH_4)_6Mo_7O_{24}\cdot 4H_2O$. No major change in band positions and profiles of the stretching modes of H_2O and NH_4^+ were observed below 70 °C. But from 75 °C, the bands at 3491 and 3329 cm^{-1} began to broaden continuously and also their intensity reduced, which signaled the onset of the dehydration process. The H_2O bands at 3491 and 3329 cm^{-1} almost disappeared at around 131 °C indicated the major dehydration process. The stretching mode of NH_4^+ at 3141 cm^{-1} broadened slightly at 121 °C and broadened appreciably and shifted to 3145 cm^{-1} at around 131 °C. With increase in temperature, that

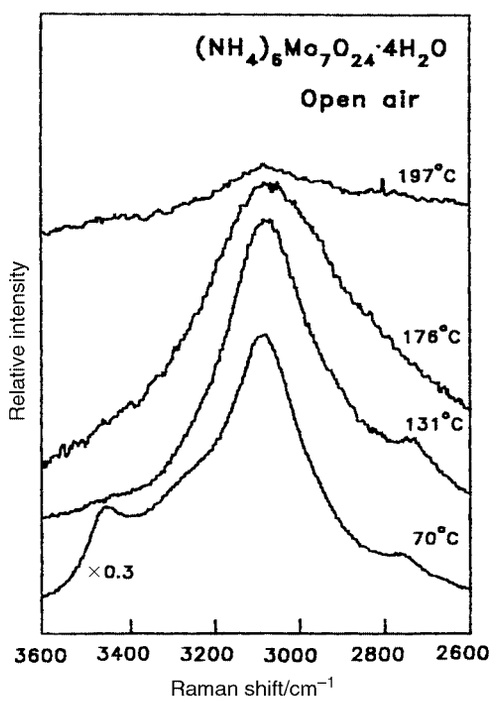

Fig. 2 Typical thermo-Raman spectra of $(NH_4)_6Mo_7O_{24}\cdot 4H_2O$ in open air from 2600 to 3600 cm^{-1} at 70, 131, 176 and 197 °C in a dynamical thermal process.

band broadened considerably from 176 °C onwards and at 197 °C it appeared as a very weak band centered at 3148 cm^{-1}. With further increase in temperature, its intensity dropped drastically from 240 °C and at around 270 °C no band corresponding to the stretching modes of NH_4^+ was visible. The characteristic spectra around 70, 131, 176 and 197 °C are shown in Fig. 2.

The spectra measured in the ν_2 and ν_4 mode regions of NH_4^+ below 100 °C showed three weak overlapped bands at 1671, 1644 and 1622 cm^{-1} along with a strong ν_4 band at 1419 cm^{-1}. The three overlapped bands broadened from 116 °C and appeared as a single broad band centered at 1661 cm^{-1} at 124 °C. Similarly, the band observed at 1419 cm^{-1} also broadened at 124 °C but their intensities did not change much. However, these bands not only broadened but their intensities also decreased after 176 °C. Around 197 °C, these bands became

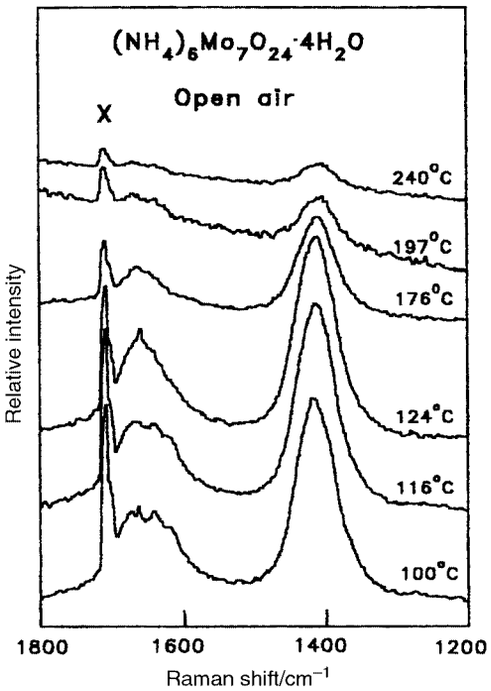

Fig. 3 Typical thermo-Raman spectra of $(NH_4)_6Mo_7O_{24}\cdot 4H_2O$ in open air from 1200 to 1800 cm^{-1} at 100, 116, 124, 176, 197 and 240 °C in a dynamical thermal process. X marks the plasma line from the laser.

very weak and indicated a major loss of NH_3. With further increase of temperature the intensity of these bands decreased and vanished around 240 °C and at around 265 °C even the ν_4 mode became invisible, which signaled another major loss of NH_3 accomplished at around 265 °C. The characteristic spectra at 100, 116, 124, 176, 197 and 240 °C are shown in Fig. 3.

Under O_2 flow

MoO_6 vibrations. In general, the major difference observed in the terminal Mo–O and bridging Mo–O–Mo stretching bands of $(NH_4)_6Mo_7O_{24}\cdot 4H_2O$ under O_2 flow compared to those in open air was the broadened nature of the bands. The typical thermo-Raman spectra measured at 25, 115, 140, 200 and 245 °C during the thermal decomposition process under O_2 flow are shown in Figs. 4(a)–(e). No major difference in spectral variation was observed from 25 to 250 °C. The spectra observed from 250 to 410 °C indicated some changes. An interesting difference was the non-appearance of the characteristic bands of MoO_3 but an increase in the intensities of the bands at 977, 917, 902 and 884 cm^{-1} corresponding to the third intermediate from 250 to 305 °C. A typical Raman spectrum measured at 275 °C is shown as Fig. 4(f). The spectra observed from 310 to 370 °C indicated an increase in the intensities of all these bands. The characteristic band of MoO_3 at around 819 cm^{-1} appeared after 310 °C and onwards. In addition to an increase in intensity, the band at 977 cm^{-1} broadened considerably with temperature and at around 350 °C a weak band at 993 cm^{-1} appeared as a shoulder to it as shown in Fig. 4(g). The gradual decrease in intensities of the medium bands at 977, 917, 902 and 884 cm^{-1} were observed from 370 °C. Around 410 °C, they disappeared completely and all the characteristic bands of MoO_3 remained. Typical thermo-Raman spectra measured at 385 and 410 °C are shown in Figs. 4(h) and 4(i), respectively.

The non-appearance of the characteristic bands of MoO_3 in the temperature range from 250 to 305 °C under O_2 flow depends upon the flow rate of O_2 in the sample cell. Under a fast flow rate of O_2, no bands corresponding to MoO_3 appeared however under slow flow rate these bands due to MoO_3 appeared as weak signals.

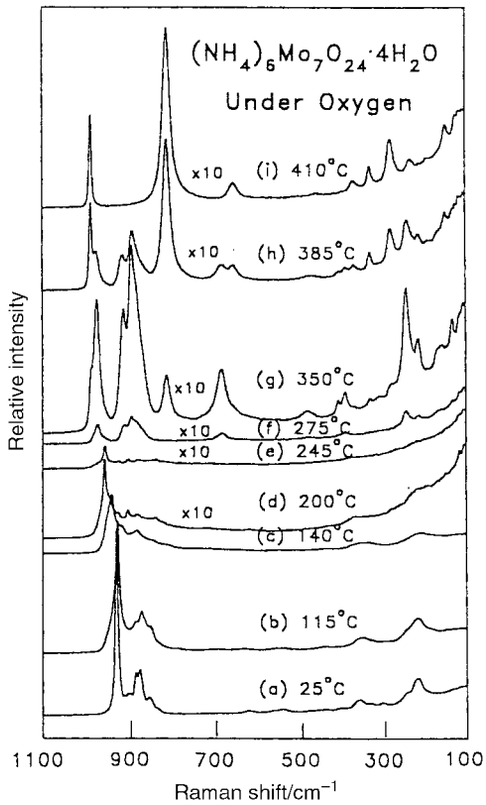

Fig. 4 Typical thermo-Raman spectra of $(NH_4)_6Mo_7O_{24}\cdot 4H_2O$ under O_2 flow in the 100 to 1100 cm^{-1} region in a dynamical thermal process. (a) $(NH_4)_6Mo_7O_{24}\cdot 4H_2O$, at room temperature, (b) $(NH_4)_6Mo_7O_{24}\cdot xH_2O$, after the onset of dehydration, (c) $11(NH_4)_2O\cdot 4(MoO_3)_7$, the first intermediate, (d) mixture of $11(NH_4)_2O\cdot 4(MoO_3)_7$, the first intermediate, and $7(NH_4)_2O\cdot 4(MoO_3)_7$, the second intermediate, (e) $7(NH_4)_2O\cdot 4(MoO_3)_7$, the second intermediate, (f) the third intermediate at 275 °C, (g) the third intermediate at 350 °C, (h) MoO_3 with the third intermediate and finally (i) MoO_3.

NH_4^+ and H_2O vibrations. The spectral variation observed in the stretching modes of H_2O and NH_4^+ and also in the ν_2 and ν_4 region of NH_4^+ under O_2 flow from 25 to 250 °C was similar to the variation observed in open air. Under open air, after 270 °C no band for NH_4^+ was visible but under O_2 flow, a band at 3145 cm^{-1} was visible from 320 °C and its intensity increased further up to 350 °C then dropped and disappeared at around 390 °C.

Under N_2 flow

The spectra observed under N_2 flow from 25 to 150 °C in the terminal Mo–O and bridging Mo–O–Mo vibration regions were similar to those in open air. Afterwards, the intensity of the overall spectrum reduced dramatically and no band was visible till 500 °C. However, when N_2 flow was replaced by O_2 flow at 380 °C arbitrarily in a dynamic thermal process, weak bands appeared from 385 °C and the spectrum observed at 390 °C showed the characteristic bands of MoO_3 along with some other intermediate. At around 450 °C, the characteristic bands of MoO_3 were quite clearly observed and the color of the sample also changed from dark purple to yellow. The spectral variation observed in the NH_4^+ and H_2O vibration regions under N_2 flow over the entire thermal process was very similar to the variation in open air.

TGA/DTA/TG-MS

The thermogravimetry (TG), differential thermogravimetry (DTG) and differential thermal analysis (DTA) thermograms of $(NH_4)_6Mo_7O_{24}\cdot 4H_2O$ measured under air flow from 25 to 500 °C with a heating rate of 5 °C min^{-1} are shown in Fig. 5. The TG thermogram showed three major weight losses of 6.85, 4.24 and 7.06% from 75 to 146 °C, from 174 to 239 °C and from 253

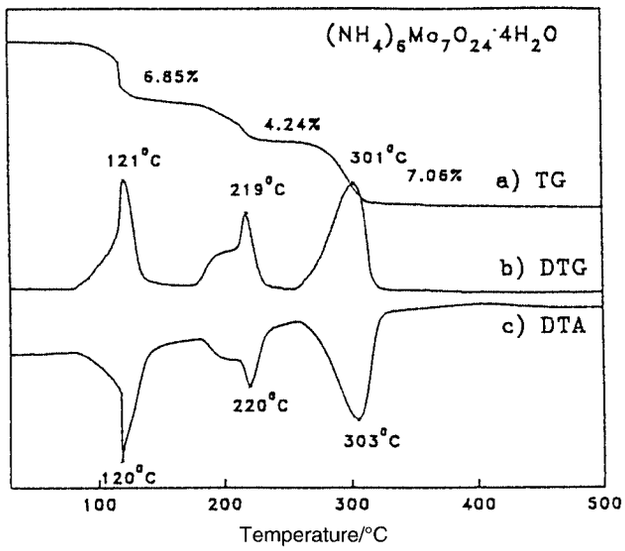

Fig. 5 (a) TG, (b) DTG and (c) DTA thermograms of $(NH_4)_6Mo_7O_{24}\cdot 4H_2O$ measured with 5 °C min^{-1} heating rate from 25 to 500 °C under a flow of air.

to 350 °C, respectively. The DTG clearly indicated a gradual weight loss in the temperature interval from 75 to 115 °C and a rapid weight loss from 116 to 146 °C in the first stage. Similarly, during the second stage, a gradual weight loss in the temperature interval from 174 to 207 °C and a rapid one from 210 to 239 °C were clear. During the third stage, the DTG thermogram indicated, in addition to the major weight loss from 253 to 307 °C, a very small fraction of weight loss in the temperature interval from 310 to 350 °C. The DTA thermogram also reflected the results of TG and DTG. The nature of the TG and DTG thermograms measured under N_2 and O_2 flow was similar to the thermograms measured under air flow.

Analysis of the gases evolved during the decomposition of $(NH_4)_6Mo_7O_{24}\cdot 4H_2O$ from 25 to 500 °C with a heating rate of 5 °C under He flow measured by a TG coupled mass spectrometer (TG-MS) reveals the formation of ions having a mass of 17 (NH_3) and 18 (H_2O) u, as illustrated in Fig. 6. The mass spectra in the range from 10 to 250 u were examined and no other significant reaction product was detected. The TG-MS trace of evolved H_2O indicated the onset of the dehydration process from 86 °C and its maximum rate at around 150 °C corresponded to the first major weight loss observed in TG. It again showed two maximum rates at 220 and 320 °C corresponding to the second and third major weight losses observed in TG. For NH_3, a minor loss at around 170 °C and two major losses at 230 and 310 °C were clearly reflected from the results of the TG-MS experiment as shown in Fig. 6. The TG-MS traces of evolved H_2O and NH_3 recorded under He flow indicated that dehydration and deammination occurred at slightly higher temperatures compared to that under air flow.

Discussion

An empirical formulae of $3(NH_4)_2O\cdot(MoO_3)_7\cdot 4H_2O$ for $(NH_4)_6Mo_7O_{24}\cdot 4H_2O$ has long been supported by crystallographic studies.[28] At room temperature six NH_4^+ are attached to Mo through O^- with ionic bonds. During heating, two NH_3 and one H_2O are evolved simultaneously, hence, it is represented by $(NH_4)_2O$. The crystal structural analysis of $(NH_4)_6Mo_7O_{24}\cdot 4H_2O$ indicated that the monoclinic unit cell contained 4 units of $(NH_4)_6Mo_7O_{24}\cdot 4H_2O$.[27] It also indicated that seven MoO_3 formed $(MoO_3)_7$ and $4(MoO_3)_7$ stabilized by $12(NH_4)_2O$ and $16H_2O$ in a unit cell. At room temperature, NH_4 attaches to Mo through O with an ionic bond. The structure of $(MoO_3)_7$ in $(NH_4)_6Mo_7O_{24}\cdot 4H_2O$ crystals was determined earlier by Lindqvist, who established a peculiar butterfly shaped configuration.[29] Later on, many crystal structural analyses were attempted in order to resolve the oxygen atoms and to refine their positions.[30–32] Evans *et al.* reported that $(NH_4)_6Mo_7O_{24}\cdot 4H_2O$ consists of seven MoO_6 octahedra condensed by edge sharing into a compact structure, which has a point symmetry $2mm$ (C_{2v}).[33] Also they mentioned that the $(MoO_3)_7$ units are assembled in layers extended normal to the y axis and in these layers $3(NH_4)_2O$ and $4H_2O$ serve to bind the molecules together by a complex system of ionic and hydrogen bonds.

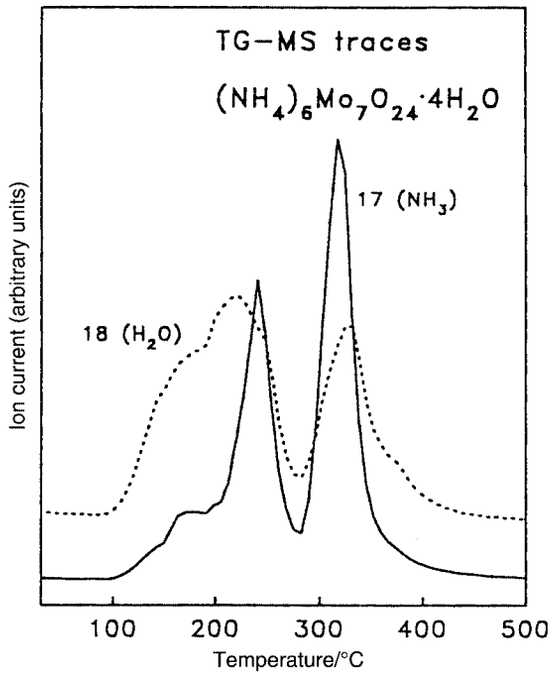

Fig. 6 TG-MS traces of evolved (----) H_2O and (—) NH_3 during the decomposition of $(NH_4)_6Mo_7O_{24}\cdot 4H_2O$ with a 5 °C min^{-1} heating rate from 25 to 500 °C under a flow of He.

In open air

In the first stage, the DTG thermogram indicated a gradual decrease in weight from 75 to 115 °C and a rapid decrease in weight at around 121 °C. In the thermo-Raman investigations, the observation of a minor decrease in intensities of the stretching bands of H_2O at 3491 and 3329 cm^{-1} from 75 to 115 °C indicated the onset of dehydration however the observation of no major change in the intensities of the ν_2 and ν_4 modes of NH_4^+ indicated that there could be no major loss of $(NH_4)_2O$. For the Mo–O mode, the strongest band at 934 cm^{-1} remained the same and the observation of only minor changes in the weak bands indicated that there was very minor modification in the structure of $(NH_4)_6Mo_7O_{24}\cdot 4H_2O$ due to the onset of dehydration. The skeleton structure of $(MoO_3)_7$ remained intact from 75 to 115 °C.

The complete disappearance of the stretching modes of H_2O and the slight decrease in intensity of the NH_4^+ stretching modes observed from 124 to 131 °C indicated the rapid loss of hydrated water along with minor loss of $(NH_4)_2O$. The appearance of a strong band at 945 cm^{-1} to replace the strong band at 934 cm^{-1} and minor variation in the weak bands at around 124 °C indicated that there could be some minor modification in the crystalline structure of $(NH_4)_6Mo_7O_{24}\cdot 4H_2O$. The complete removal of hydrated water and the partial removal of $(NH_4)_2O$ gave the first intermediate with no change in the skeleton structure of $(MoO_3)_7$.

During the second stage weight loss, the DTG thermogram clearly indicated a gradual weight loss from 174 to 207 °C and a rapid weight loss from 210 to 239 °C. The DTA thermogram also reflected the observation made with TG and DTG over that temperature interval. In the thermo-Raman spectra, the

observation of a continuous decrease in the intensities of the stretching and ν_2 and ν_4 modes of NH_4^+ from 176 °C indicated a major loss of $(NH_4)_2O$. An interesting spectral variation observed in the Mo–O stretching region was the appearance and increase in intensity of the strong band at 961 cm^{-1} from 176 °C and the simultaneous decrease in intensity of the band at 945 cm^{-1}. The disappearance of the band at 945 cm^{-1} revealed the vanishing of the first intermediate. This spectral variation indicated the formation of the second intermediate. Although there was some modification in the crystalline structure due to the major release of $(NH_4)_2O$ over this temperature interval, the skeleton structure of $(MoO_3)_7$ was not perturbed.

During the third stage, the TG and DTG thermograms indicated a major loss of weight from 253 to 307 °C and another very small fraction of weight loss from 310 to 350 °C. In the thermo-Raman spectra, the complete disappearance of the bands of NH_4^+ at around 265 °C indicated major loss of $(NH_4)_2O$. Because of the weak nature of the NH_4^+ modes, the intensity of the NH_4^+ bands dropped drastically immediately subsequent to the loss of the remaining $(NH_4)_2O$, starting at around 255 °C, hence it was not possible to follow this stage completely till 307 °C in the thermo-Raman spectra. The appearance of the characteristic band of MoO_3 at 993 cm^{-1} and the decrease in intensity of the strong band at 961 cm^{-1} were observed from 255 °C onwards. The spectral variation observed in the terminal Mo–O and bridging Mo–O–Mo stretching regions clearly indicated the dramatic change in the structure of $(MoO_3)_7$, which began to break down to MoO_3 at around 255 °C. Although the characteristic bands of MoO_3 appeared after 255 °C and their intensity increased with temperature, the appearance of the weak bands at 977, 917, 902 and 884 cm^{-1} together indicated the presence of the third intermediate along with a small amount of MoO_3. The decrease in intensities of those weak bands from 310 °C onwards, their complete disappearance and the presence of only the characteristic bands of MoO_3 after 347 °C indicated the loss of the third intermediate and formation of MoO_3 after 347 °C. The characteristic bands of MoO_3 became stronger and sharper above 350 °C because crystal grains were growing continuously with temperature.

The appearance of the strong terminal Mo–O bands at 945 and 961 cm^{-1} at around 124 and 199 °C, respectively, clearly indicated the formation of two stable intermediates during the thermal decomposition. Till 250 °C, the intensity of the terminal Mo–O stretching band was very strong compared to other bands in that region, but afterwards as soon as MoO_3 started to appear, as expected, the band observed at 819 cm^{-1} corresponding to MoO_3 became quite strong, which signaled the breakdown of $(MoO_3)_7$ to form MoO_3. The complicated layer structure of MoO_3 was interpreted as being built up by distorted MoO_6 octahedron.[34] Julien *et al.* have reported that MoO_3 exhibits an intriguing layered structure consisting of double layers of MoO_6 octahedra.[35] The present thermo-Raman investigation indicated that during the thermal decomposition process from 25 to 250 °C, $(MoO_3)_7$ distorted slightly and the collapse of $(MoO_3)_7$ occurred to form MoO_3 immediately subsequent to the loss of the remaining volatile compounds at 255 °C. Although the process of collapse of $(MoO_3)_7$ started at 255 °C, it was not completed until around 347 °C. The presence of small amounts of residual volatile compounds during this temperature interval might delay the complete collapse of all $(MoO_3)_7$ to MoO_3 and hence the third intermediate (might be mixed molybdena with residual volatile compounds) appeared along with MoO_3 over this temperature interval. The disappearance of the weak bands at 977, 917, 902 and 884 cm^{-1} of the third intermediate and the appreciable increase in intensities of characteristic bands of MoO_3 at 993 and 819 cm^{-1} above 350 °C indicated the increase in concentration of MoO_3.

The spectral variations observed in the thermo-Raman spectra, the weight losses observed in TG, the DTA thermograms and the results from the TG-MS experiment suggest that the thermal decomposition could follow the sequence shown in Scheme 1 based on $4[3(NH_4)_2O{\cdot}(MoO_3)_7{\cdot}4H_2O]$ in a unit cell.

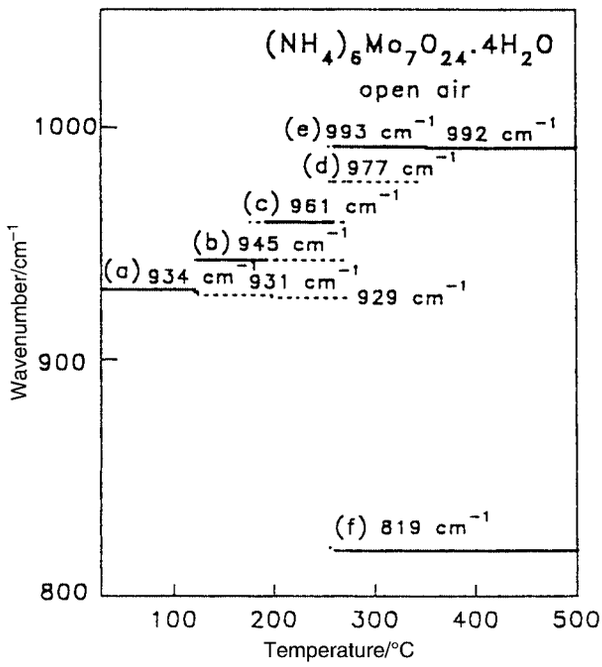

Fig. 7 Band positions of some strong bands observed in the 800 to 1000 cm^{-1} region during the decomposition of $(NH_4)_6Mo_7O_{24}{\cdot}4H_2O$ with 5 °C min^{-1} heating rate from 25 to 500 °C in open air.

The band positions of the symmetric stretching vibration of strong terminal Mo–O bands measured during the dynamic thermal process from 25 to 500 °C in open air is presented in Fig. 7 for the range from 800 to 1000 cm^{-1}. The band at 934 cm^{-1} appeared as the strongest band in the temperature interval from 25 to 123 °C, which indicated no major change in the skeleton structure of $(MoO_3)_7$ over this temperature interval. Another terminal Mo–O stretching band at 945 cm^{-1} started to appear from 121 °C and became the strongest band in that region from 124 to 192 °C indicating the existence of the first intermediate. Similarly, another band at 961 cm^{-1} started to appear from 176 °C and became the strongest from 193 to 259 °C indicating the presence of the second intermediate. The bands at 977 (Fig. 7(d)), 993 (Fig. 7(e)) and 819 cm^{-1} (Fig. 7(f)) appeared from 255 °C onwards. The band at 819 cm^{-1} (Fig. 7(f)) corresponding to MoO_3 turned out to be the strongest band from 260 °C onwards, which signaled the breakdown of $(MoO_3)_7$ to form MoO_3. The band at 977 cm^{-1} appeared along with the characteristic bands of MoO_3 from 255 to 350 °C indicating the coexistence of the third intermediate with MoO_3. From Fig. 7 the evolution of $(MoO_3)_7$ can be traced step by step dynamically from the original compound through the first intermediate, to the second intermediate, to the mixture of the third intermediate with MoO_3 and finally to the decomposed product MoO_3.

Under O_2 flow

Under O_2 flow, the weight losses observed in the TG during the first two stages were the same as in air flow, but in the third stage the temperature interval for the final fraction of weight loss extended up to 400 °C. An interesting difference observed under O_2 flow from 250 to 305 °C was the non-appearance of the characteristic band for MoO_3 but the increase in the intensities of the bands at 977, 917, 902 and 884 cm^{-1} corresponded to the third intermediate. The dominance of these bands in the terminal Mo–O and bridging Mo–O–Mo stretching regions and the band observed at 3145 cm^{-1} from 330 to 350 °C indicated the presence of the third intermediate (might be some

First stage from 75 to 146 °C

$$4[3(NH_4)_2O{\cdot}(MoO_3)_7{\cdot}4H_2O] \longrightarrow 11(NH_4)_2O{\cdot}4(MoO_3)_7 + 16\ H_2O\uparrow + 2NH_3\uparrow + H_2O\uparrow$$

Experimental weight loss = 6.85%

Calculated weight loss = 6.88%

In this stage, sixteen hydrated H_2O and one $(NH_4)_2O$ lost.

First intermediate $11(NH_4)_2O{\cdot}4(MoO_3)_7$.

Second stage from 174 to 239 °C

$$11(NH_4)_2O{\cdot}4(MoO_3)_7 \longrightarrow 7(NH_4)_2O{\cdot}4(MoO_3)_7 + 8\ NH_3\uparrow + 4\ H_2O\uparrow$$

Experimental weight loss = 4.24%

Calculated weight loss = 4.21%

In this stage, four $(NH_4)_2O$ lost.

Second intermediate $7(NH_4)_2O{\cdot}4(MoO_3)_7$.

Third stage from 253 to 350 °C

$$7(NH_4)_2O{\cdot}4(MoO_3)_7 \longrightarrow 28\ MoO_3 + 14\ NH_3\uparrow + 7\ H_2O\uparrow$$

Experimental weight loss = 7.06%

Calculated weight loss = 7.37%

In this stage, the remaining $7(NH_4)_2O$ lost.

Final product MoO_3 derived.

Scheme 1

mixed molybdena with residual volatile components) as the dominant species in this high temperature range under O_2 flow. Although the process of removal of the final residual amount of volatile compounds started at around 260 °C it took a longer time to reach completion, hence the process of collapse of $(MoO_3)_7$ to MoO_3 took longer. The bands corresponding to the third intermediate, mixed molybdena, appeared dominant in the terminal Mo–O and bridging Mo–O–Mo stretching regions of the thermo-Raman spectra. Immediately subsequent to the loss of the residual volatile compounds at around 410 °C the intensities of the characteristic bands of MoO_3 increased and appeared distinctively.

Under N_2 flow

The thermo-Raman investigation on the thermal decomposition of $(NH_4)_6Mo_7O_{24}{\cdot}4H_2O$ under N_2 flow in the terminal Mo–O, bridging Mo–O–Mo, NH_4^+ and H_2O vibration regions indicated that the decomposition in the temperature interval from 25 to 150 °C was similar to that in open air. Afterwards from 150 °C, no band was visible in the terminal Mo–O and bridging Mo–O–Mo vibration regions but the spectral variation observed in the NH_4^+ and H_2O vibration regions was similar to that observed in open air. The non-observation of any band in the terminal Mo–O and bridging Mo–O–Mo vibration might be because an O_2 deficient sample was a poor Raman scatterer and absorbed the incident laser light and the scattered light due to its dark purple color.

Conclusion

The spectral variation of $(NH_4)_6Mo_7O_{24}{\cdot}4H_2O$ observed in the thermo-Raman investigations in open air indicated the gradual removal of hydrated water over the temperature interval 75 to 115 °C and the rapid loss of hydrated water along with the loss of one $(NH_4)_2O$ at around 124 to 131 °C. The thermo-Raman investigations and the results of TG, DTA and TG-MS experiments strongly suggested that the first intermediate formed after the complete removal of hydrated water along with one $(NH_4)_2O$ could be $11(NH_4)_2O{\cdot}4(MoO_3)_7$. The results of the present investigation also indicated the loss of four $(NH_4)_2O$ from the first intermediate resulting in the second intermediate $7(NH_4)_2O{\cdot}4(MoO_3)_7$ over the temperature interval 174 to 239 °C. The thermo-Raman investigations detected the formation of MoO_3 along with the third intermediate (mixed molybdena along with some residual volatile compounds) at around 255 °C. A simultaneous increase in the intensity of MoO_3 and a decrease in the intensity of the coexisting third intermediate were observed from 310 to 347 °C and pure MoO_3 was derived above 350 °C. The thermo-Raman investigations strongly suggest that $(NH_4)_6Mo_7O_{24}{\cdot}4H_2O$ consists of a $(MoO_3)_7$ unit stabilized by $3(NH_4)_2O$ and $4H_2O$ and also indicated the presence of $(NH_4)_2O$ along with $(MoO_3)_7$ till 250 °C because all of the Raman spectra were similar, consisting of a strong band with several weak ones. The step-by-step decomposition clearly indicated that the water and ammonia in the $(NH_4)_6Mo_7O_{24}{\cdot}4H_2O$ crystals are bonded to $(MoO_3)_7$ in slightly different strengths because the strongest Raman band showed only a slight shift in position. The present investigations clearly indicated that $(MoO_3)_7$ in $(NH_4)_6Mo_7O_{24}{\cdot}4H_2O$ during the thermal decomposition process remained intact till 250 °C and the collapse of $(MoO_3)_7$ occurred to form MoO_3 immediately subsequent to the loss of the remaining volatile compounds at 255 °C.

The thermal decomposition of $(NH_4)_6Mo_7O_{24}{\cdot}4H_2O$ observed under O_2 flow from 25 to 250 °C was similar to that

in open air. The spectral variations observed after 250 °C suggested a slightly different decomposition pathway. An interesting difference observed under O_2 flow was the appearance of the third intermediate (mixed molybdena with residual volatile compounds) as the dominant species over the temperature interval 260 to 370 °C. Subsequently, MoO_3 was derived only at elevated temperatures above 400 °C. The thermal decomposition of $(NH_4)_6Mo_7O_{24}\cdot 4H_2O$ under N_2 flow over the temperature interval 25 to 150 °C was very similar to that in open air. However, the non-observation of any band in the terminal Mo–O and bridging Mo–O–Mo vibration regions in the thermo-Raman spectra after 150 °C might be because of O_2 deficient conditions.

In all, these thermo-Raman investigations have detected the intermediates, nature of the intermediates, existence temperature ranges of the intermediates and also the temperature at which pure MoO_3 was derived during the decomposition of $(NH_4)_6Mo_7O_{24}\cdot 4H_2O$ in open air and under O_2 and N_2 flow dynamically. The present study revealed new information on the thermal decomposition of $(NH_4)_6Mo_7O_{24}\cdot 4H_2O$ at a molecular level and the results will be useful for further studies on supported molybdena catalysts.

Acknowledgements

Mr Anil Ghule and Mr Chetan Bhongale are thanked for their technical assistance. This work was supported by the National Science Council of the Republic of China (NSC-88-CPC-M-007–002 and NSC-89–2113-M007–013).

References

1 G. Centi and F. Trifiro, *Chem. Rev.*, 1988, **88**, 55.
2 K. Y. S. Ng and E. Gulari, *J. Catal.*, 1985, **92**, 340.
3 C. Li, H. Zhang, K. Wang, Y. Miao and Q. Xin, *Appl. Spectrosc.*, 1993, **47**, 56.
4 C. C. Williams, J. G. Ekerdt, J. M. Jehng, F. D. Hardcastle, A. M. Turek and I. E. Wachs, *J. Phys. Chem.*, 1991, **95**, 8781.
5 J. A. R. van Veen, P. A. J. M. Hendriks, E. J. G. M. Romers and R. R. Andrea, *J. Phys. Chem.*, 1990, **94**, 5275.
6 N. S. Chieu, S. H. Bauer and M. F. Johnson, *J. Catal.*, 1986, **98**, 32.
7 A. N. Desikan, L. Huang and S. T. Oyama, *J. Phys. Chem.*, 1991, **95**, 10050.
8 J. C. Edwards, R. D. Adams and P. D. Ellis, *J. Am. Chem. Soc.*, 1990, **112**, 349.
9 D. S. Kim, K. Segawa, T. Soeya and I. E. Wachs, *J. Catal.*, 1992, **136**, 539.
10 D. S. Kim, Y. Kurusu, I. E. Wachs, F. D. Hardcastle and K. Segawa, *J. Catal.*, 1989, **120**, 325.
11 C. C. Williams, J. G. Ekerdt, J. M. Jehng, F. D. Hardcastle, A. M. Turek and I. E. Wachs, *J. Phys. Chem.*, 1991, **95**, 8781.
12 M. Inoue, A. Kurusu, H. Wakamatsu and T. Inui, *Appl. Catal.*, 1987, **32**, 203.
13 E. Ma, *Bull. Chem. Soc. Jpn.*, 1964, **37**, 171.
14 E. Ma, *Bull. Chem. Soc. Jpn.*, 1964, **37**, 648.
15 L. Erdey, S. Gal and G. Liptay, *Talanta*, 1964, **11**, 913.
16 Y. Zhoulan, Z. Qinsheng and C. Shaoyi, *Zhongnan Kuangye Xueyuan Xuebao*, 1993, **24**, 541.
17 Y. Zhoulan, L. Xinhai and C. Qiyuam, *Thermochim. Acta*, 2000, **352**, 107.
18 A. Kiss and P. Gado, *Acta Chim. Hung.*, 1970, **66**, 235.
19 H. Chang and P. J. Huang, *Anal. Chem.*, 1997, **69**, 1485.
20 H. Chang and P. J. Huang, *J. Raman Spectrosc.*, 1998, **29**, 97.
21 H. Chang, P. J. Huang and S. C. Hou, *Mater. Chem. Phys.*, 1999, **58**, 12.
22 R. Murugan, P. J. Huang, A. Ghule and H. Chang, *Thermochim. Acta*, 2000, **346**, 83.
23 R. Murugan, A. Ghule and H. Chang, *J. Appl. Phys.*, 1999, **86**, 6779.
24 R. Murugan, A. Ghule and H. Chang, *J. Phys. Condens. Matter*, 2000, **12**, 677.
25 R. Murugan, A. Ghule, C. Bhongale and H. Chang, *J. Mater. Chem.*, 2000, **10**, 2157.
26 K. Nakamoto, *Infrared and Raman Spectra of Inorganic and Co-ordination Compounds*, Wiley, New York, 1986.
27 F. D. Hardcastle and I. E. Wachs, *J. Raman Spectrosc.*, 1990, **21**, 683.
28 J. H. Sturdivant, *J. Am. Chem. Soc.*, 1937, **59**, 630.
29 I. Lindqvist, *Ark. Kemi*, 1950, **2**, 325.
30 E. Shimao, *Bull. Chem. Soc. Jpn.*, 1967, **40**, 1609.
31 H. T. Evans, *J. Am. Chem. Soc.*, 1968, **90**, 3275.
32 B. M. Gatehouse and P. Leverett, *Chem. Commun.*, 1968, 901.
33 H. T. Evans, B. M. Gatehouse and P. Leverett, *J. Chem. Soc., Dalton Trans.*, 1975, 505.
34 N. Wooster, *Z. Kristallogr.*, 1931, **80**, 504.
35 C. Julien, B. Yebka and G. A. Nazri, *Mater. Sci. Eng. B*, 1996, **38**, 65.